

# Multilayer Heterogeneous Membrane Biosensor Based on Multiphysical Field Coupling for Human Serum Albumin Detection

Haoyu Wang, Pengli Xiao, Shengbo Sang, Honglie Chen, Xiushan Dong, Yang Ge, Xing Guo, and Dong Zhao\*



Cite This: *ACS Omega* 2023, 8, 3423–3428



Read Online

ACCESS |



Metrics & More

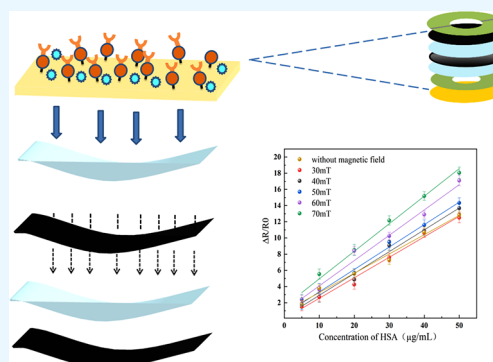


Article Recommendations



Supporting Information

**ABSTRACT:** A factor closely associated with renal disease status in clinical diagnosis is abnormal human serum albumin (HSA) concentration levels in human body fluids urine, serum, etc. The surface stress biosensor was developed as a new type of biosensor to detect protein molecule concentration and has a wide range of clinical applications. However, further sensitivity improvement is required to achieve higher detection performance. Herein, MXene/PDMS/Fe<sub>3</sub>O<sub>4</sub>/PDMS of the multilayer heterogeneous membrane biosensor (MHBios) based on the coupling of the magnetic field, electric field, and surface stress field was successfully developed to achieve high sensitivity HSA detection through magnetic sensitization. The modified antibody specifically binds to HSA at the AuNP layer, allowing the biosensor to convert the surface stress caused by PDMS film deformation into an electrical signal. When the biosensor was exposed to a uniform magnetic field, the conductive path of the conductive layer was reshaped further as the magnetic force amplified the deformation of the PDMS film, enhancing the conversion of biological signals to electrical signals. The results exhibited that the detection limit (LOD) of the MHBios was 78 ng/mL when HSA concentration was 0–50  $\mu\text{g}/\text{mL}$ , which was markedly lower than the minimum diagnostic limit of microalbuminuria. Furthermore, the MHBios detected HSA in actual samples, confirming the potential for early disease screening.



## 1. INTRODUCTION

Kidney disease is a major concern because of its extremely high mortality rate and the complexity of detecting it early. Early detection can dramatically improve the effectiveness of disease treatment and prevention.<sup>1–3</sup> Microalbuminuria is a critical biomarker for assessing chronic kidney disease (CKD). The potency of human serum albumin (HSA) present in normal human urine is 20 mg/mL<sup>-1</sup>. If the HSA in urine exceeds the upper limit of this value, the risk of kidney disease is indicated.<sup>4</sup> Hence, efficient detection of urinary HSA concentration can effectively diagnose and prevent kidney disease at an early stage,<sup>3–5</sup> and it is necessary to design a biosensor that can effectively detect the concentration of HSA.

These days, platforms for HSA detection and sensing have been developed, including radioimmunoassay, immunoturbidimetry, high-performance liquid chromatography (HPLC), and urine test paper colorimetry.<sup>5–7</sup> In the past, urine test paper colorimetry was developed for HSA detection. Low sensitivity and semiquantitative methods led to inaccurate and false-positive results, though.<sup>8–10</sup> High sensitivity and accuracy were obtained by immunoturbidimetry, HPLC, and radioimmunoassay for the detection of HSA, but their broad applicability was constrained by laborious sample pretreatment procedures. Additionally, the price of the equipment was high.<sup>11</sup> The surface stress-based membrane biosensor (MBios)

has shown improvements over existing sensors in terms of price, detection speed, and operability. Hence, the MBios has received a lot of attention recently as a reliable technique for HSA detection.<sup>9,12–15</sup>

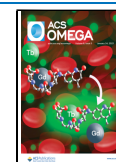
The MBios is a novel type of biosensor that converts surface stress produced during biomolecular detection into physically detectable signals to enable biomolecule analysis.<sup>16</sup> However, for the purpose of improving the performance of detecting higher single molecules, the sensitivity of the MBios needed to be further improved.<sup>16,17</sup>

As a consequence, we built a magnetic electrocoupling-based very sensitive biosensor. The influence of the magnetic field was intensified by the creation of multilayer heterostructure membranes, increasing the sensitivity of sensor detection. We did a thorough comparison of the biosensor with the existing biosensors that detect HSA and were able to identify various HSA concentrations in various situations. Ultimately, the biosensor was utilized to detect actual human urine samples in

**Received:** November 15, 2022

**Accepted:** December 22, 2022

**Published:** January 9, 2023



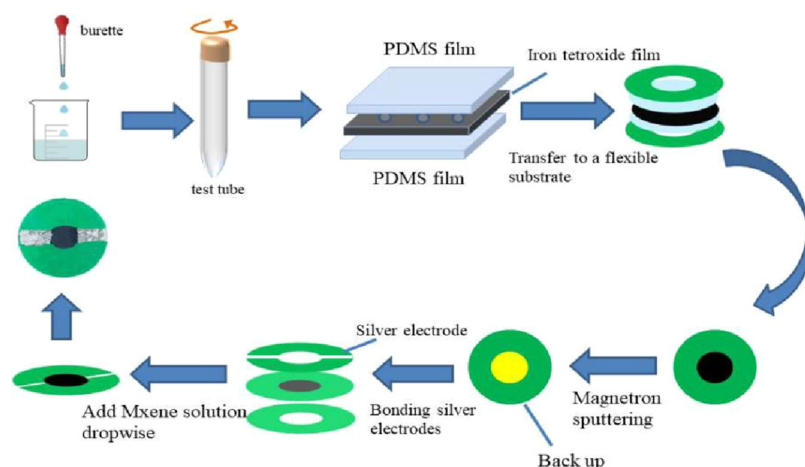


**Figure 1.** MHBios preparation process. At the end of the preparation flow chart is the real MHBios picture.

order to assess its usability, and the results indicated that it had the potential to be used in the adjunct diagnosis of renal illnesses.

## 2. MATERIALS AND METHODS

**2.1. Materials for Preparation.** PDMS (polydimethylsiloxane) was manufactured by Dow Corning (Midland, MI). PAA (03326 polyacrylic acid) was produced by an American polasciences company. PAA concentration is 25%, molecular weight is 345,000, pH value is 2–3, and Brinell viscosity is 682c PS. Cysteamine (CYS) was provided by Aladdin (Shanghai, China).  $\text{Fe}_3\text{O}_4$  particles were dispersed in alcohol solution by an ultrasonic disperser. Carcinoembryonic antigen (CEA) was obtained from Sangon Biotech (Shanghai, China). BSA (bovine serum albumin) was produced by Bioengineering (Shanghai, China). Tau protein (microtubule-associated protein) was manufactured by Bioengineering (Shanghai, China). Gelatin was purchased from McLean Biochemical Technology Co, Ltd. (Shanghai, China). The HSA antibody (anti-HSA) and HSA were purchased from Haling Biology (Shanghai, China). The gold target used for magnetron sputtering was purchased from Deyang ona Co., Ltd. (Sichuan, China).

**2.2. Preparation of the MHBios.** The glass substrate was first cleaned with acetone, isopropanol, ethanol, and deionized water, followed by hydrophilic modification with an oxygen plasma cleaning machine (Atto, Beijing Zhongxing Bairui Technology Co., Ltd). Polyacrylic acid (PAA, 66.7%) with deionized water solvent was spin-coated on glass at 3500 rpm for 1 min and cured at 120 °C for 15 min to take the shape of the PAA membrane. When the PDMS prepolymer was mixed with the hardener at a 10:1 weight ratio, a deaerator (KK-300SSE, Kurabo, Japan) was used to eliminate air bubbles from the mixed solution. The PDMS mixture was coated on the PAA membrane and heated at 2000 rpm for 60 s and 120 °C for 15 min to prepare the PDMS membrane. The  $\text{Fe}_3\text{O}_4$  nanoparticles were fully dispersed into alcohol for 8 min with an ultrasonic dispersant (Nanjing Shunma Instrument Equipment Co., Ltd.) at a ratio of 0.05 g/mL. The  $\text{Fe}_3\text{O}_4$  membrane was manufactured by coating the  $\text{Fe}_3\text{O}_4$  mixture on PDMS membranes at 3500 rpm for 1 min and curing at 60 °C for 15 min.<sup>18</sup> The sandwich composite membranes were fabricated by spin-coating PDMS on the  $\text{Fe}_3\text{O}_4$  membrane at 3000 rpm for 1 min and cured at 100 °C for 30 min. After this, the PDMS/

$\text{Fe}_3\text{O}_4$ /PDMS sandwich composite membranes were transferred from the glass substrate to polyethylene terephthalate (PET). PET was sputtered with a AuNP layer by a magnetron sputtering machine (Hefei Kejing Material Technology Co, Ltd. VTC-600-2HD, China).<sup>19</sup> The MXene membrane was formed by coating the MXene mixture on the other side of PET at 3000 rpm for 1 min and heated at 80 °C for 10 min.<sup>20</sup> The conductive silver adhesive was imprinted on PET to convert electrical signals (Figure 1).

**2.3. Characterization.** The electrical characteristics of the MHBios was measured by a digital multimeter (Keithley 2400, Tektronix, Shanghai, China). A dual target magnetron sputtering instrument (VTC-600-2HD, Kejing Material Technology Co, Ltd., Hefei, China) was served to sputter AuNP layers on the surface. The surface morphology of the MHBios was characterized by a scanning electron microscope (geminiSEM 300, Germany). A magnetic field generator (pem-60, China) is used to produce a strength of 30–70 mT for the uniform magnetic field. Using energy-dispersive spectroscopy (EDS) observation, the MHBios surface was modified to form the corresponding chemical bonds, and validation modification was successful.

## 3. RESULTS AND DISCUSSION

**3.1. Characterizations of the MHBios.** To enable the HSA molecules to be caught by the MHBios specificity, the antibodies were altered.<sup>21</sup> Scanning electron microscopy (SEM) and EDS were used to demonstrate the effective modification of antibodies. SEM was employed to describe the MHBios surface before antibodies were modified (Figure S2a). SEM was then applied to describe the surface of the MHBios after the change of antibodies, revealing that the antibodies were dispersed uniformly across the surface of the AuNP layer (Figure S2b).<sup>31–33</sup> EDS was intended to show the MHBios surface in the detection process in order to further explain the element changes before and after in the character of the MHBios during the modification process. Only C, O, Si, and Au elements were present on the surface of the MHBios membranes prior to alteration, as shown by the EDS scanning image (Figure S2c). The presence of the S element served as evidence that the CYS molecule was successfully modified on the AuNP-PDMS membrane. The surface of the modified AuNP-PDMS membrane also had more C and O elements and formed a new element N because anti-HSA and HSA are

protein molecules (Figure S2d). The thickness of each layer in the multilayer heterogeneous membrane structure, as well as the profile morphology of the MHBios, was subsequently determined by SEM (Figure S3).

### 3.2. Analysis of the MHBios Signal Conversion

**Principle.** Electrical conductivity is quite high in the two-dimensional (2D) transition metal compound MXene, which consists of carbon/nitrogen/carbon. MXene has exceptional sensing capabilities due to its high electrical conductivity. MXene was consequently selected as the conductive layer material for the MHBios. The MHBios' resistance modifies with the deformation of the MXene membrane.<sup>16,17,22</sup> Surface stress was produced by the specific binding of anti-HSA and HSA to the sensitive layer. Surface tension caused the MXene membrane's structure to alter, which changed the conductive route through the membrane.<sup>23,24</sup> Additionally, the magnetic nanoparticles move on the MHBios surface under the influence of a uniform magnetic field as a result of magnetic Fe<sub>3</sub>O<sub>4</sub> sensitization. This causes the PDMS membrane to deform more, which shortens the conductive route and increases resistance. After the addition of HSA droplets, the surface stress caused by antigen-specific binding amplified the deformation, resulting in a decreased conduction path and an increased relative resistance ( $\Delta R/R_0$ ) of the MXene membrane. Then, by capturing different concentrations of HSA, the MHBios produced greater relative resistance changes with the increase in HSA concentration, to improve the detection performance of the sensor. The MHBios then caused significant changes in relative resistance with the continual growth of the magnetic field by altering the size of various magnetic fields (Figure S3). Because of this, the MHBios was able to magnetically sensitize and improve its sensitivity in multifield coupling.

**3.3. HSA Detection of the MHBios.** For the sake of better detecting HSA, the performance of the MHBios was tested in advance. At room temperature, the MHBios' reaction to the influence of several conditions was investigated. On the AuNP layer, various weights of deionized water were applied and left for 10 min. Because of the surface stress brought on by water's gravity, the MXene membrane distorted, changing the relative resistance (Figure 2). Furthermore, HSA was detected by the MHBios under the nonuniform magnetic field and

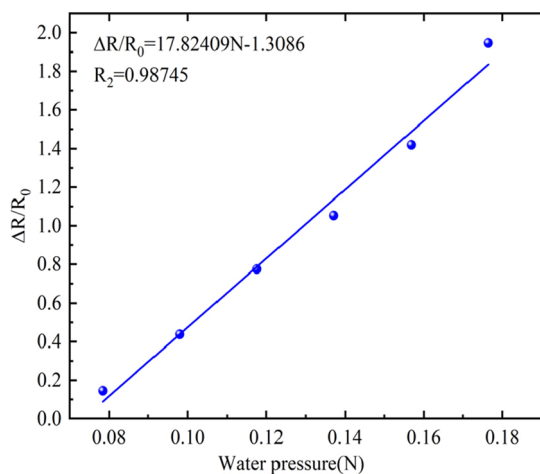


**Figure 2.** Deionized water was placed on the MHBios to detect the change of surface stress on the relative resistance of the sensor when the control voltage was 5 V.

generated a linear relationship in the range of 10–50  $\mu\text{g/mL}$  (Figure 3a). The linear equation used was  $\Delta R/R_0 = 0.27894 C_{\text{HSA}} - 1.25345$  ( $R^2 = 0.99349$ ). The detection limit (LOD) of the MHBios was computed by the formula  $\text{LOD} = 3\sigma/S$  as 0.53  $\mu\text{g/mL}$ .<sup>2,25–27</sup>

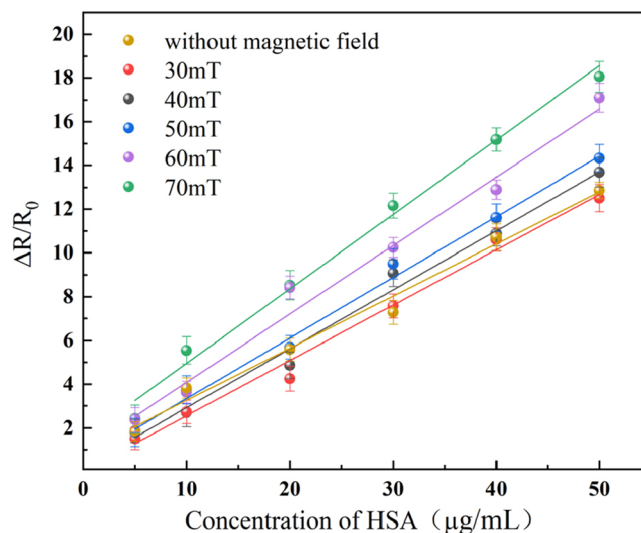


**Figure 3.**  $\Delta R/R_0$  detected by the MHBios. The test was repeated for five times under the same experimental conditions.

A homogenous magnetic field of varying intensities was used to further evaluate the impact of magnetic fields on sensor detection and to see if the MHBios would perform at a higher level. The MHBios was put into a uniform magnetic field for 10 min. The change in relative resistance of the MHBios in the magnetic field was detected, which determined that the optimal influence range of the magnetic field is 30–70 mT. The MHBios additionally demonstrated a linear response to various HSA concentrations under various magnetic field intensities (Figure 3b). Under a magnetic field strength of 70 mT, the sensitivity of the MHBios is the highest (Figure S5). The linear equation  $\Delta R/R_0 = 0.31274 C_{\text{HSA}} + 0.02075$  ( $R^2 = 0.98272$ ) was obtained in a 70 mT magnetic field. The calculated MHBios detection limit (LOD) for a uniform magnetic field is 78 ng/mL, which is orders of magnitude less than the LOD for no uniform magnetic field. The MHBios were made with various levels of Fe<sub>3</sub>O<sub>4</sub>, and the optimal concentration of Fe<sub>3</sub>O<sub>4</sub> was determined to be 0.05 g/mL in the presence of an optimum magnetic field and a perfect HSA concentration (Figure S6). A magnetic field of 70 mT was delivered to the MHBios every 10 min while it was being tested with an HSA solution that contained 50 g/mL concentration. The fact that the sensitivity of MHBios remained mostly unaltered throughout each time period suggests that the magnetic field action time had minimal impact on MHBios sensitivity (Figure S7). The MHBios reaction was augmented by magnetic Fe<sub>3</sub>O<sub>4</sub> nanoparticles under the influence of the magnetic field created by the surface stress, proving that magnetic sensitization successfully increased the MHBios' sensitivity.

By contrasting the MHBios with other biosensors from the prior literature, the detection performance of the MHBios was demonstrated.<sup>2,11,28</sup> The LOD of the MHBios was many orders of magnitude lower than those of the NiFe<sub>2</sub>O<sub>4</sub>/paper-based magnetoelastic biosensor, fluorescent probe sensor, and

**Table 1. Performance Comparison of Various Biosensors for HSA Detection**

| material   | method  | detection range ( $\mu\text{g/mL}$ ) | LOD ( $\mu\text{g/mL}$ ) | labels     | sample collection time | ref.      |
|--|---|--------------------------------------|--------------------------|------------|------------------------|-----------|
| novel $\text{NiFe}_2\text{O}_4$ /Paper                       | magnetoelastic effect of $\text{NiFe}_2\text{O}_4$ nanoparticles and mechanical properties of the paper   | 10–200                               | 0.43                     | label-free | immediate              | 4         |
| antibody-functionalized gold nanorods                        | surface plasmon resonance characteristics and sensitivity of antibody-functionalized gold nanorods (GNRs) | 30–300                               | 1                        | label-free | immediate              | 5         |
| water-soluble BODIPY-based fluorescent probe                 | spectral methods and molecular docking  | 0–8.35                               | 50                       | label-free | immediate              | 32        |
| a fluorescent sensor recognized by the FA1 site              | HSA-selective light-up fluorescent sensor, DCM-ML   | 0–80                                 | 250                      | label-free | immediate              | 2         |
| MXene/PDMS/ $\text{Fe}_3\text{O}_4$ /AuNP composite membrane | MHBios based on MSEC enhancement  | 0–50                                 | 0.078                    | label-free | immediate              | this work |

antibody-functionalized gold nanorod sensor, all of which have wider detection ranges than the MHBios.<sup>29,30</sup> The MHBios not only has no label and is less expensive than the water-soluble BODIPY-based fluorescent probe but also offers higher sensitivity. Consequently, the MHBios has a lot of promise for identifying HSA (Table 1).

**3.4. Specificity of the MHBios.** Different latent interference factors, including those with the same concentrations of HSA, BSA, CEA, glucose, T protein, glucose oxidase, and gelatin, were investigated to express the specificity of the MHBios (Figure 4). The response of the MHBios was

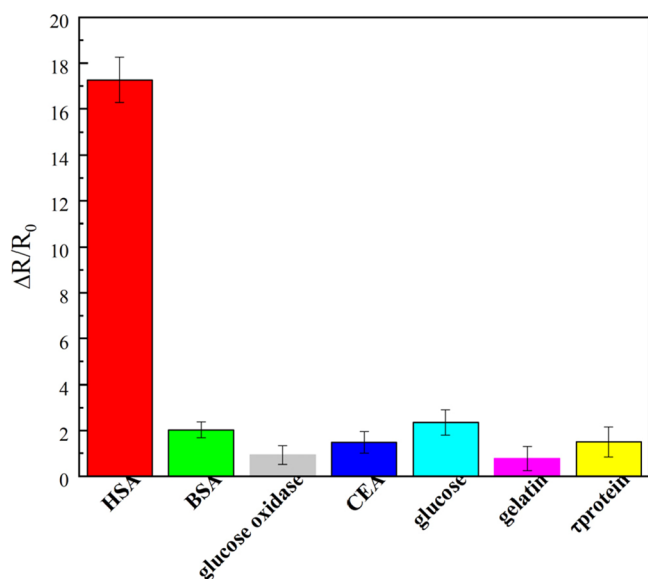


**Figure 4.** Specificity of the MHBios was determined. Five parallel experiments were carried out.

more pronounced when HSA was detected, indicating that the MHBios has relatively high specificity for HSA detection. This is due to the anti-HSA specificity combined with HSA molecules produced by the surface stress of the reaction. Because of other biological molecules and the MHBios between physical adsorption, the reaction is relatively weak.

**3.5. Stability of the MHBios.** Additionally, stability, a crucial aspect of the MHBios, was evaluated. The MHBios was created and kept at a temperature of 4 °C. The MHBios was used to test HSA, BSA, T protein, gelatin solution, and glucose solution at 50  $\mu\text{g/mL}$  (Figure 5). The MHBios detected the activity of HSA through the response of chart results  $\Delta R/R_0$ , which remained relatively stable during the test for a while, indicating that the MHBios has significant stability. In

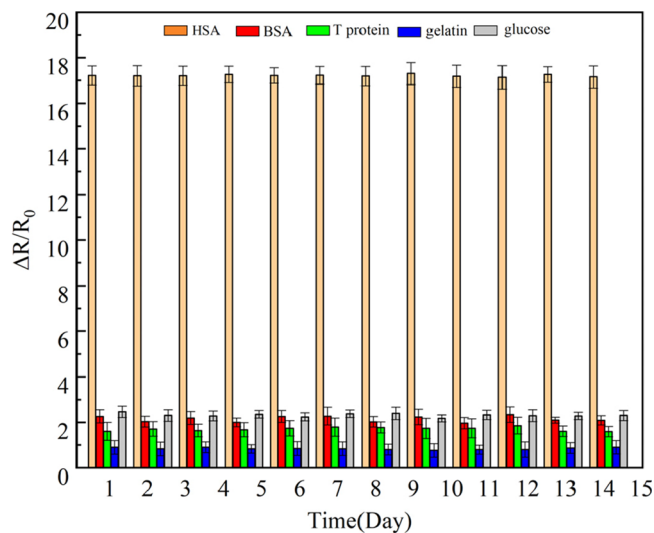


**Figure 5.** MHBios tested the stability of HSA at a concentration of 50  $\mu\text{g/mL}$ .

conclusion, it was anticipated that the excellent stability of the MHBios will eventually offer an auxiliary diagnosis for renal illness.

**3.6. Selectivity of the MHBios.** Evaluation of MHBios selectivity was carried out through the detection of the MHBios selectivity to HSA in a complex environment. The different solutions were mixed and drip-added to the MHBios. The MHBios was rinsed five times to get rid of any leftover molecules after 20 min of reaction, shielding it from the impacts of sample viscosity or proton conductivity. It is worth noting that different signals were shown only in the solution containing HSA. Moreover, the presence of T protein and glucose oxidase had no obvious response to the MHBios (Figure 6). The MHBios nonetheless retained high selectivity for HSA detection in complicated situations as a result.

**3.7. Detection of Clinical Samples.** To validate the reliability of the MHBios in complex environments, human urine was quantified at room temperature. Samples were provided by Shanxi Bethune Hospital. A sample of initial human urine with various HSA concentrations was chosen and quantified as drops onto the MHBios. The MHBios detection performance of clinical samples is shown in Table 2. The recovery rate of the MHBios fluctuated in the range of 87.7 and 108.8, indicating that for MHBios detection in a complex environment, HSA has higher reliability.

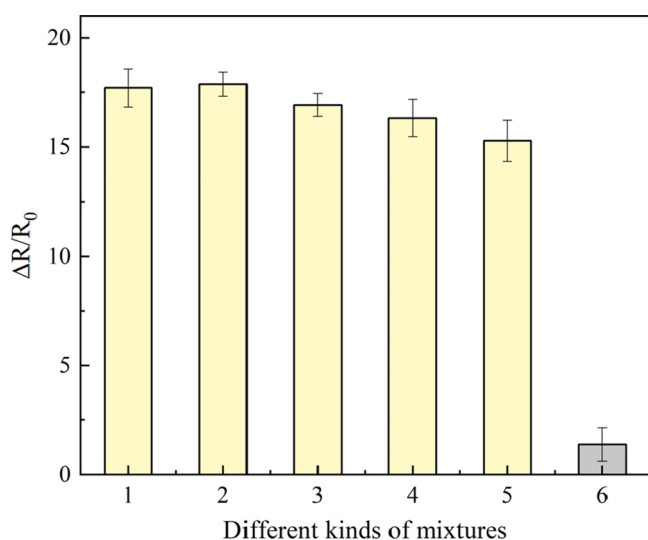


**Figure 6.** Selectivity of the MHBios: 1 stands for HSA solution; 2 represents the solution consisting of HSA and BSA; 3 represents the solution consisting of HSA, CEA, and BSA; 4 represents the solution consisting of HSA, gelatin, and glucose; 5 represents the whole mixture; and 6 represents the solution consisting of T protein and glucose oxidase. Five parallel experiments were carried out.

**Table 2.** Detect HSA Concentration in Human Urine

| samples | original<br>[ $\mu\text{g}/\text{mL}^{-1}$ ] | found<br>[ $\mu\text{g}/\text{mL}^{-1}$ ] | recovery<br>[%] | SD<br>[ $\mu\text{g}/\text{mL}^{-1}$ ] |
|---------|--|---|-----------------|--|
| 1       | 5.7  | 5.06                                      | 88.8            | 0.35                                   |
| 2       | 38   | 37.81                                     | 99.7            | 0.84                                   |
| 3       | 46   | 41.76                                     | 90.8            | 0.51                                   |
| 4       | 44   | 45.32                                     | 103.4           | 0.46                                   |
| 5       | 43   | 46.78                                     | 108.8           | 0.82                                   |
| 6       | 76   | 66.65                                     | 87.7            | 0.97                                   |

#### 4. CONCLUSIONS

In general, the MHBios was reported to realize the effective conversion from biological signals to surface stress and magnetic force on MXene/PDMS/ $\text{Fe}_3\text{O}_4$ /PDMS composite membranes. The coupling of surface stress and magnetic force fundamentally improved the sensitivity of surface stress biosensors. Additionally, it can perform sensitive HSA detection. The PDMS membrane deforms more rapidly than the  $\text{Fe}_3\text{O}_4$  membrane under the influence of the magnetic field, amplifying the surface stress that can be output as electrical impulses. Therefore, multiphysical field coupling enhancement is realized. Under the uniform magnetic field, the MHBios showed good detection performance. The detection limit of the MHBios without the magnetic field has been greatly reduced thanks to the application of a multilayer heterostructure, where the LOD of the MHBios is 78 ng/mL. Especially in the actual sample test, the MHBios has high reliability, which indicates that the MHBios has a potential application value in the auxiliary diagnosis of kidney disease.

#### ■ ASSOCIATED CONTENT

##### SI Supporting Information

The Supporting Information is available free of charge at <https://pubs.acs.org/doi/10.1021/acsomega.2c07338>.

The modification process of anti-HSA, the characterization of the MHBios by SEM and EDS, the

deformation process of the MXene membrane under different magnetic fields, the detection and determination of the optimal magnetic field intensity of HSA, the detection and determination of the optimal concentration of  $\text{Fe}_3\text{O}_4$  in the MHBios, and the effect of magnetic field addition time on the sensitivity of the MHBios (PDF)

#### ■ AUTHOR INFORMATION

##### Corresponding Author

**Dong Zhao** – Shanxi Key Laboratory of Micro Nano Sensors & Artificial Intelligence Perception, College of Information and Computer, Taiyuan University of Technology, Taiyuan 030024, China; [orcid.org/0000-0002-0382-4561](https://orcid.org/0000-0002-0382-4561); Email: [zhaodong01@tyut.edu.cn](mailto:zhaodong01@tyut.edu.cn)

##### Authors

**Haoyu Wang** – Shanxi Key Laboratory of Micro Nano Sensors & Artificial Intelligence Perception, College of Information and Computer, Taiyuan University of Technology, Taiyuan 030024, China

**Pengli Xiao** – Shanxi Key Laboratory of Micro Nano Sensors & Artificial Intelligence Perception, College of Information and Computer, Taiyuan University of Technology, Taiyuan 030024, China

**Shengbo Sang** – Shanxi Key Laboratory of Micro Nano Sensors & Artificial Intelligence Perception, College of Information and Computer, Taiyuan University of Technology, Taiyuan 030024, China; [orcid.org/0000-0003-3011-7632](https://orcid.org/0000-0003-3011-7632)

**Honglie Chen** – Shanxi Key Laboratory of Micro Nano Sensors & Artificial Intelligence Perception, College of Information and Computer, Taiyuan University of Technology, Taiyuan 030024, China

**Xiushan Dong** – Shanxi Bethune Hospital, Taiyuan 030024, China

**Yang Ge** – Shanxi Key Laboratory of Micro Nano Sensors & Artificial Intelligence Perception, College of Information and Computer, Taiyuan University of Technology, Taiyuan 030024, China

**Xing Guo** – Shanxi Key Laboratory of Micro Nano Sensors & Artificial Intelligence Perception, College of Information and Computer, Taiyuan University of Technology, Taiyuan 030024, China

Complete contact information is available at:

<https://pubs.acs.org/10.1021/acsomega.2c07338>

##### Notes

The authors declare no competing financial interest.

#### ■ ACKNOWLEDGMENTS

The authors are grateful for the support by the Basic Research Program of Shanxi for Youths (No. 20210302124557, 20210302124429, and 20210302124164), the National Natural Science Foundation of China (Nos. 51975400 and 61703298), and the Science and Technology Innovation Program of Colleges and Universities in Shanxi Province (Study on stress-magnetic biosensor of MXene-PDMS composite membrane coupled with nano magnetic probe).

## REFERENCES

- (1) Allarakha, S.; Dixit, K.; Zaheer, M. S.; Siddiqi, S. S.; Moinuddin, A. A.; Ali, A. Levels of anti-fructose-modified HSA antibodies correlate with disease status in diabetic subjects. *Int. J. Biol. Macromol.* **2016**, *88*, 93.
- (2) Chao, X.; Yao, D.; Qi, Y.; Yuan, C.; Huang, D. A fluorescent sensor recognized by the FA1 site for highly sensitive detection of HSA. *Anal. Chim. Acta* **2021**, *1188*, No. 339201.
- (3) Shaikh, M. O.; Zhu, P. Y.; Wang, C. C.; Du, Y. C.; Chuang, C. H. Electrochemical immunosensor utilizing electrodeposited Au nanocrystals and dielectrophoretically trapped PS/Ag/ab-HSA nanoprobe for detection of microalbuminuria at point of care. *Biosens. Bioelectron.* **2019**, *126*, 572.
- (4) Zhang, Q.; Dong, Z.; Dong, X.; Duan, Q.; Ji, J.; Liu, Y.; Pei, Z.; Ji, C.; Sang, S. Double-Side-Coated Grid-Type Mechanical Membrane Biosensor Based on AuNPs Self-assembly and 3D Printing. *Adv. Mater. Interfaces* **2021**, *9*, No. 2101461.
- (5) Kordasht, H. K.; Saadati, A.; Hasanzadeh, M. A flexible paper based electrochemical portable biosensor towards recognition of ractopamine as animal feed additive: Low cost diagnostic tool towards food analysis using aptasensor technology. *Food Chem.* **2022**, *373*, No. 131411.
- (6) Li, P.; Wang, Y.; Zhang, S.; Xu, L.; Wang, G.; Cui, J. An ultrasensitive rapid-response fluorescent probe for highly selective detection of HSA. *Tetrahedron Lett.* **2018**, *59*, 1390.
- (7) Nishitani, S.; Sakata, T. Enhancement of Signal-to-Noise Ratio for Serotonin Detection with Well-Designed Nanofilter-Coated Potentiometric Electrochemical Biosensor. *ACS Appl. Mater. Interfaces* **2020**, *12*, 14761–14769.
- (8) Nithyayini, K. N.; Harish, M. N. K.; Nagashree, K. L. Electrochemical detection of nitrite at NiFe<sub>2</sub>O<sub>4</sub> nanoparticles synthesised by solvent deficient method. *Electrochim. Acta* **2019**, *317*, 701.
- (9) Shu, J.; Tang, D. Recent Advances in Photoelectrochemical Sensing: From Engineered Photoactive Materials to Sensing Devices and Detection Modes. *Anal. Chem.* **2020**, *92*, 363.
- (10) Wang, L.; Meng, T.; Zhao, D.; Jia, H.; An, S.; Yang, X.; Wang, H.; Zhang, Y. An enzyme-free electrochemical biosensor based on well monodisperse Au nanorods for ultra-sensitive detection of telomerase activity. *Biosens. Bioelectron.* **2020**, *148*, No. 111834.
- (11) Xu, H.; Shen, G.; Peng, C.; Han, X.; Duan, L.; Cheng, T. BODIPY-based fluorescent probe for selective detection of HSA in urine. *Dyes Pigments* **2022**, *197*, No. 109915.
- (12) Xu, W.; Sakran, M.; Fei, J.; Li, X.; Weng, C.; Yang, W.; Zhu, G.; Zhu, W.; Zhou, X. Electrochemical Biosensor Based on HRP/Ti<sub>3</sub>C<sub>2</sub>/Nafion membrane for Determination of Hydrogen Peroxide in Serum Samples of Patients with Acute Myocardial Infarction. *ACS Biomater. Sci. Eng.* **2021**, *7*, 2767–2773.
- (13) Zhao, D.; Zhang, Q.; Zhang, Y.; Liu, Y.; Pei, Z.; Yuan, Z.; Sang, S. Sandwich-type Surface Stress Biosensor Based on Self-Assembled Gold Nanoparticles in PDMS membrane for BSA Detection. *ACS Biomater. Sci. Eng.* **2019**, *5*, 6274.
- (14) Kowalczyk, A. Trends and perspectives in DNA biosensors as diagnostic devices. *Curr. Opin. Electrochem.* **2020**, *23*, 36.
- (15) Erdogan, Z. O.; Kucukkolbasi, S. Fabrication of an electrochemical biosensor based on Fe<sub>3</sub>O<sub>4</sub> nanoparticles and uricase modified carbon paste electrode for uric acid determination. *Monatsh Chem.* **2021**, *152*, 309.
- (16) Sang, S.; Feng, Q.; Tang, X.; Wang, T.; Huang, X.; Jian, A.; Ma, Z.; Zhang, W. PDMS micro-membrane capacitance-type surface stress biosensors for biomedical analyses. *Microelectron. Eng.* **2015**, *134*, 33.
- (17) Osica, I.; Melo, A. F. A. A.; Lima, F. C. D. A.; Shiba, K.; Imamura, G.; Crespilho, F. N.; Betlej, J.; Kurzydowski, K. J.; Yoshikawa, G.; Ariga, K. Nanomechanical Recognition and Discrimination of Volatile Molecules by Au Nanocages Deposited on Membrane-Type Surface Stress Sensors. *ACS Appl. Nano Mater.* **2020**, *3*, 4061–4068.
- (18) Zhao, Y.; Huo, D.; Jiang, L.; Zhou, S.; Yang, M.; Hou, C. Synthesis of dopamine-derived N-doped carbon nanotubes/Fe<sub>3</sub>O<sub>4</sub> composites as enhanced electrochemical sensing platforms for hydrogen peroxide detection. *Microchim. Acta* **2020**, *187*, 605.
- (19) Ren, C.; Bayin, Q.; Feng, S.; Fu, Y.; Ma, X.; Guo, J. Biomarkers detection with magnetoresistance-based sensors. *Biosens. Bioelectron.* **2020**, *165*, No. 112340.
- (20) Xu, X.; Chen, Y.; He, P.; Wang, S.; Ling, K.; Liu, L.; Lei, P.; Huang, X.; Zhao, H.; Cao, J.; Yang, J. Wearable CNT/Ti<sub>3</sub>C<sub>2</sub>Tx MXene/PDMS composite strain sensor with enhanced stability for real-time human healthcare monitoring. *Nano Res.* **2021**, *14*, 2875.
- (21) Zhou, J.; Zeng, Y.; Wang, X.; Wu, C.; Cai, Z.; Gao, B. Z.; Gu, D.; Shao, Y. The capture of antibodies by antibody-binding proteins for ABO blood typing using SPR imaging-based sensing technology. *Sens. Actuators B: Chem.* **2020**, *304*, No. 127391.
- (22) Xin, M.; Li, J.; Ma, Z.; Pan, L.; Shi, Y. MXenes and Their Applications in Wearable Sensors. *Front. Chem.* **2020**, *8*, 297.
- (23) Khorsandifard, M.; Jafari, K.; Sheikhalah, A. A Proposal for a Novel Surface-Stress Based BioMEMS Sensor Using an Optical Sensing System for Highly Sensitive Diagnoses of Bio-particles. *Sens. Imaging* **2021**, *22*, 35.
- (24) He, W.; Sohn, M.; Ma, R.; Kang, D. J. Flexible single-electrode triboelectric nanogenerators with MXene/PDMS composite membrane for biomechanical motion sensors. *Nano Energy* **2020**, *78*, No. 105383.
- (25) Russell, S. M.; de la Rica, R. Paper transducers to detect plasmon variations in colorimetric nanoparticle biosensors. *Sens. Actuators, B* **2018**, *270*, 327–332.
- (26) Eickenberg, B.; Meyer, J.; Helmich, L.; Kappe, D.; Auge, A.; Weddemann, A.; Wittbracht, F.; Hutten, A. Lab-on-a-Chip Magneto-Immunoassays: How to Ensure Contact between Superparamagnetic Beads and the Sensor Surface. *Biosensors* **2013**, *3*, 327.
- (27) Friedman, A. N.; Fadem, S. Z. Reassessment of albumin as a nutritional marker in kidney disease. *J. Am. Soc. Nephrol.* **2010**, *21*, 223.
- (28) Ksenofontov, A. A.; Bocharov, P. S.; Ksenofontova, K. V.; Antina, E. V. Water-Soluble BODIPY-Based fluorescent probe for BSA and HSA detection. *J. Mol. Liq.* **2022**, *345*, No. 117031.
- (29) Guo, X.; Liu, R.; Li, H.; Wang, J.; Yuan, Z.; Zhang, W.; Sang, S. A Novel NiFe<sub>2</sub>O<sub>4</sub>/Paper-Based Magnetoelastic Biosensor to Detect Human Serum Albumin. *Sensors* **2020**, *20*, 5286.
- (30) Mirjalili, S.; Tohidi Moghadam, T.; Sajedi, R. H. Facile and Rapid Detection of Microalbuminuria by Antibody-Functionalized Gold Nanorods. *Plasmonics* **2022**, *17*, 1269.
- (31) Guntupalli, R.; Lakshmanan, R. S.; Hu, J.; Huang, T. S.; Barbaree, J. M.; Vodyanoy, V.; Chin, B. A. Rapid and sensitive magnetoelastic biosensors for the detection of Salmonella typhimurium in a mixed microbial population. *J. Microbiol. Methods* **2007**, *70*, 112.
- (32) Lakhera, P.; Chaudhary, V.; Jha, A.; Singh, R.; Kush, P.; Kumar, P. Recent developments and fabrication of the different electrochemical biosensors based on modified screen printed and glassy carbon electrodes for the early diagnosis of diverse breast cancer biomarkers. *Mater. Today Chem.* **2022**, *26*, No. 101129.
- (33) Eissa, S.; Tlili, C.; L'Hocine, L.; Zourob, M. Electrochemical immunosensor for the milk allergen beta-lactoglobulin based on electrografting of organic film on graphene modified screen-printed carbon electrodes. *Biosens. Bioelectron.* **2012**, *38*, 308.